

# Thermally Stable Hydrogen Compounds Obtained under High Pressure on the Basis of Carbon Nanotubes and Nanofibers

I. O. Bashkin<sup>1,\*</sup>, V. E. Antonov<sup>1</sup>, A. V. Bazhenov<sup>1</sup>, I. K. Bdikin<sup>1</sup>, D. N. Borisenko<sup>1</sup>,  
E. P. Krinichnaya<sup>2</sup>, A. P. Moravsky<sup>2</sup>, A. I. Harkunov<sup>1</sup>, Yu. M. Shul'ga<sup>2</sup>,  
Yu. A. Ossipyan<sup>1</sup>, and E. G. Ponyatovsky<sup>1</sup>

<sup>1</sup> Institute of Solid-State Physics, Russian Academy of Sciences, Chernogolovka, Moscow region, 142432 Russia

\*e-mail: bashkin@issp.ac.ru

<sup>2</sup> Institute of Problems of Chemical Physics, Russian Academy of Sciences,  
Chernogolovka, Moscow region, 142432 Russia

Received February 3, 2004

Compounds containing 6.3–6.5 wt % H and thermally stable in vacuum up to 500°C were obtained by annealing graphite nanofibers and single-walled carbon nanotubes in hydrogen atmosphere under a pressure of 9 GPa at temperatures up to 450°C. A change in the X-ray diffraction patterns indicates that the crystal lattice of graphite nanofibers swells upon hydrogenation and that the structure is recovered after the removal of hydrogen. It was established by IR spectroscopy that hydrogenation enhances light transmission by nanomaterials in the energy range studied (400–5000 cm<sup>-1</sup>) and results in the appearance of absorption bands at 2860–2920 cm<sup>-1</sup> that are characteristic of the C–H stretching vibrations. The removal of about 40% of hydrogen absorbed under pressure fully suppresses the C–H vibrational peaks. The experimental results are evidence of two hydrogen states in the materials at room temperature; a noticeable portion of hydrogen forms C–H bonds, but the most of the hydrogen is situated between the graphene layers or inside the nanotubes. © 2004 MAIK “Nauka/Interperiodica”.

PACS numbers: 61.46.+w; 61.48.+c; 62.50.+p; 78.30.Na

The interaction of carbon nanostructural materials with gaseous hydrogen has been intensively studied over the last five years. The developed surface of these materials causes a considerable applied interest aimed at producing hydrogen accumulators and reducing the consumption of organic fuel in modern industry. For the academic studies, of interest is the character of hydrogen interaction with carbon nanotubes and nanofibers. In the published works, the saturation of nanostructures with hydrogen was carried out under relatively mild conditions; the hydrogen pressure did not exceed 100–120 atm (10–12 MPa) at liquid nitrogen or room temperature (see, e.g., review [1]). The data of different authors on the maximal amount of accumulated hydrogen show a scatter of two orders of magnitude, from several tenths to several tens of H wt %. As the general rule, the processes of hydrogen absorption and release in the cycles of pressure buildup and reduction were found to be reproducible at both room and nitrogen temperatures. Based on the data on the hydrogen absorption and release as functions of pressure or temperature, most authors assume that physisorption of H<sub>2</sub> molecules on the graphene layers is the dominating mechanism of hydrogen absorption. The studies of physical properties are few in number. The results of recent measurements of electronic transport properties and Raman spectra of single-walled nanotubes during the course of hydrogen adsorption and

desorption at pressures up to 8 atm and temperatures from 4 to 500 K [2] are in accordance with the assumption about hydrogen physisorption. The maximal hydrogen content in nanotubes subjected to deep purification exceeded 6 wt % at pressures from 2 to 20 atm and a temperature of 77 K [2].

The chemical potential of hydrogen increases under pressure, and there are many examples of the increase in hydrogen solubility or the formation of hydride phases in the metal–hydrogen systems at high pressures. In this work, the interaction of hydrogen with carbon nanostructures—graphite nanofibers (GNFs) and single-walled carbon nanotubes (SWNTs)—is studied upon the thermal treatment with maximal parameters of 9 GPa and 450°C. The treatment gave samples that contained up to 7 wt % H and differed from the nanostructures hydrogenated under mild conditions by a higher thermal stability: the main hydrogen mass was released at  $T \geq 500^\circ\text{C}$ .

Starting GNFs were synthesized in a direct-flow quartz reactor in a CO : H<sub>2</sub> = 4 : 1 gas mixture at 600°C for 6 h using a mixed Fe : Cu = 7 : 3 catalyst. Scanning electron microscopy showed that the GNF length was, on the average, 30 μm and the diameter ranged from 100 to 300 nm. The content of graphite nanofiber in the prepared material was about 90%.

Carbon black containing 15–20% SWNT was synthesized by the electric arc method in helium atmosphere at a pressure of 0.86 atm using a metallic Co : Ni = 3 : 1 catalyst [3]. To remove impurities from SWNT, carbon black was subjected to ultrasonic treatment in a concentrated hydrochloric acid, and then to the multistage treatment with hydrochloric acid alternating with oxidation in air at temperatures up to 540°C. The content of single-walled nanotubes in the product was estimated using scanning and transmission electron microscopies and was found to be equal to 50–60%.

In the experiments, a GNF or SWNT sample with a mass of about 60 mg was placed in a high-pressure chamber and saturated with hydrogen obtained by thermal decomposition of  $\text{AlH}_3$ . The sample was held under a hydrogen pressure of 9 GPa first for 18 h at  $T = 350^\circ\text{C}$  and then for another 6 h at  $450^\circ\text{C}$ . At the end of holding, the chamber was cooled to  $-140^\circ\text{C}$  and unloaded to atmospheric pressure at this temperature. Then, the hydrogen-saturated material was taken out from the chamber and further held in liquid nitrogen. This technique was described in more detail in [4], where it was used to hydrogenate  $\text{C}_{60}$  fullerite.

From the hydrogenated GNF and SWNT powders, samples with a mass of several milligrams were chosen to determine their thermal stability and hydrogen content and to study them by X-ray diffraction and IR spectroscopy.

To estimate the thermal stability, the sample in a liquid nitrogen bath was placed in a nonhermetic copper container, while the latter was placed in a quartz ampoule that was cooled from outside by liquid nitrogen. The ampoule was attached to a vacuum system with the calibrated volume, the system was pumped out to a pressure of  $10^{-3}$  mmHg, and the ampoule was heated at a rate of 20 K/min, with simultaneous measurement of the pressure  $P$  of a gas released during the course of heating to 600–650°C. The sample mass was determined by weighing after measurements.

The typical manometric curves for GNF-H and SWNT-H are shown in Fig. 1. The right axis of the graph indicates the amount  $x$  of liberated hydrogen as calculated under the assumption that the gas consisted only of  $\text{H}_2$  molecules. The  $x(T)$  dependences for GNF-H and SWNT-H are closely similar to each other. In the interval from 77 K to  $0^\circ\text{C}$ , the amount of liberated gas increases with temperature rather slowly, a small jump is observed near  $0^\circ\text{C}$ , and the gas release is terminated near room temperature. The total amount of hydrogen released upon heating to room temperature is 0.15–0.5 wt %. Gas is virtually not evolved from the samples upon heating from room temperature to  $450^\circ\text{C}$ , but the second stage of intense release begins near  $500^\circ\text{C}$ , and about 5 wt % H is collected at 600–650°C, i.e., an order of magnitude greater than upon heating to room temperature. The rate of gas release is low, so that the process is not terminated up to 600–650°C, and, as is shown in Fig. 1 by the example of GNF-H, an addi-

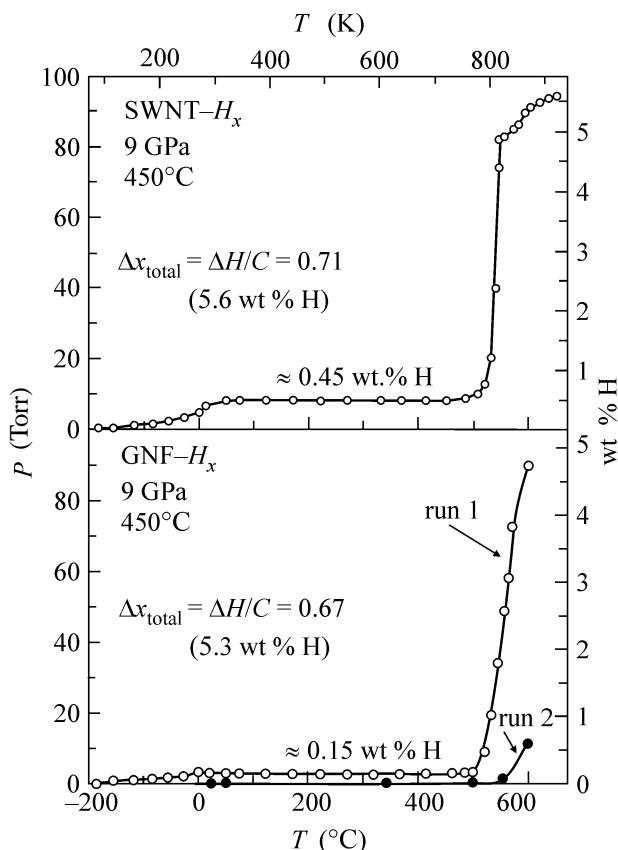


**Fig. 1.** Temperature dependence of gas pressure in a preliminarily evacuated volume (left vertical scale) and its recalculation into the amount of hydrogen evolved from the sample (right scale) upon heating at a rate of 20 K/min for single-walled carbon nanotubes (SWNT) and graphite nanofibers (GNF; two heating cycles) saturated with hydrogen at a pressure of 9 GPa and temperatures up to  $450^\circ\text{C}$ .

tional amount of gas is liberated upon repeated sample heating to  $600^\circ\text{C}$  at the same rate.

To determine the total hydrogen content and estimate the composition of liberated gas, the hydrogenated GNF and SWNT samples heated to room temperature were burned out in an oxygen flow at  $1400^\circ\text{C}$  and the combustion products  $\text{H}_2\text{O}$  and  $\text{CO}_2$  were weighed. These measurements gave  $x = 6.3$  wt % H for GNF and  $x = 6.8$  wt % H for SWNT (this corresponds to the chemical formulas  $\text{CH}_{0.81}$  and  $\text{CH}_{0.88}$ , respectively), with a spread in data less than  $\pm 0.05$  wt %. The data obtained agree satisfactorily with the estimate  $x \approx 5$  wt % H derived from the gas release between room temperature and  $650^\circ\text{C}$ , if it is considered that the gas release was incomplete. Such an agreement is evidence that hydrogen was liberated predominantly in the form of  $\text{H}_2$  molecules rather than of hydrocarbons (e.g., if methane  $\text{CH}_4$  were released, the amount of its molecules and, correspondingly, pressure would be twice as low in the gas-release experiments). A comparison of the burning results with the gas-release data allows the con-

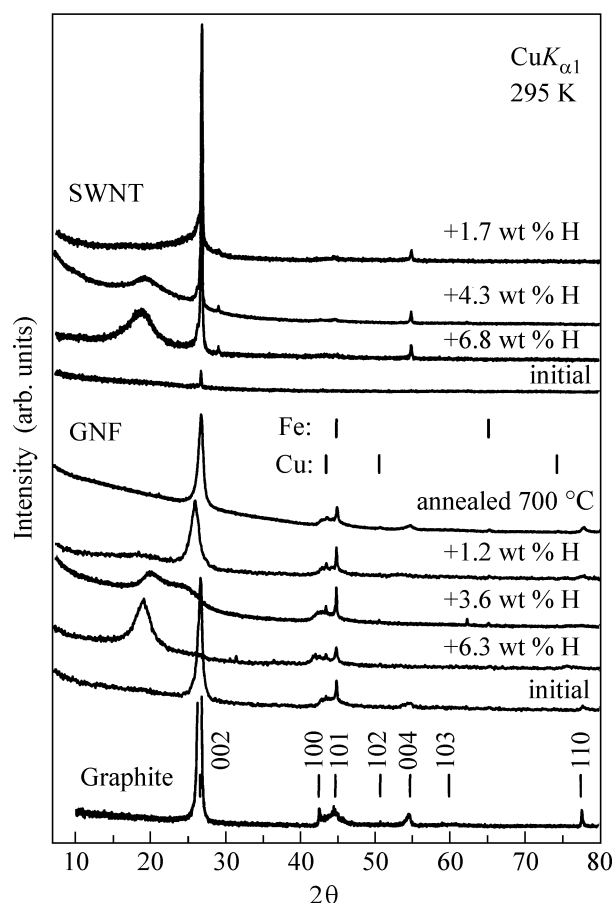


**Fig. 2.** X-ray diffraction patterns of single-walled carbon nanotubes and graphite nanofibers: in the initial state, after saturation with hydrogen at 9 GPa (6.8 and 6.3 wt % H, respectively), after removal of about 40% of absorbed hydrogen (4.3 and 3.6 wt % H), after degassing annealing to 600–650°C (1.7 and 1.2 wt % H), and after prolonged annealing at 700°C (GNF). For comparison, the diffraction pattern of a GDG-6 graphite powder is also shown. Bar diagrams of Fe and Cu indicate the catalyst admixture in GNF. Room temperature.

clusion to be drawn that, after measurements with heating to 600–650°C presented in Fig. 1, about 1.2 and 1.7 wt % H remained in the GNF and SWNT samples, respectively.

Figure 2 shows the X-ray diffraction patterns of GNFs and SWNTs in the initial and hydrogenated states and after various annealing procedures. Partial annealing with the removal of ~40% of hydrogen absorbed under pressure (the residual contents were 3.6 wt % H in GNF and 4.3 wt % H in SWNT) was carried out by holding the sample in an evacuated volume at a temperature of about 500°C, until the pressure of released gas reached the calculated value. Annealing of a GNF at 700°C was performed in a dynamic vacuum of  $<10^{-5}$  mmHg for 6 h. The X-ray diffraction pattern of the ground high-density graphite GDG-6 is presented in Fig. 2 for comparison. Measurements were made at

room temperature on a D500 Siemens diffractometer with the monochromatized  $\text{CuK}_{\alpha 1}$  radiation.

The diffraction patterns of initial GNFs include a strong reflection near the graphite (002) line at  $2\Theta = 26.5^\circ$ , a number of weak reflections near the other graphite lines, and the lines of catalyst components. After the saturation of a GNF with hydrogen, a broad intense peak appears near  $19^\circ$  instead of a very strong graphite reflection, while the other graphite reflections undergo a marked shift to small angles, and only the catalyst lines do not change their positions. After two heating cycles to 600°C shown in Fig. 1, the peak at  $19^\circ$  disappears and the diffraction pattern mainly regains its initial shape. Nevertheless, the most intense reflection remains markedly shifted to small angles, in agreement with the fact that hydrogen is removed incompletely. A prolonged vacuum annealing at 700°C results in a complete recovery of the initial diffraction pattern. A comparison of the diffraction pattern of the sample having 3.6 wt % H after partial annealing with the diffraction patterns of the extreme states shows that it represents the diffraction pattern of a two-phase state, in which the strongest reflections are shifted toward each other ( $2\Theta \approx 19.9^\circ$  and  $24.0^\circ$ ) and are strongly broadened.

In the diffraction pattern of the initial SWNTs, no reflections are seen from the nanotubes (a weak reflection can be, in principle, observed at small angles ( $2\Theta \sim 6^\circ$ ) because of the triangular SWNT packing in beams; see, e.g., [5]). A sharp weak reflection at the position of the graphite (002) line should be caused by the presence of an admixture of graphitized particles in the material. The catalyst reflections are not seen. After the hydrogenation of an SWNT, a broad peak appears near  $18.5^\circ$ , while the narrow graphite (002) and (004) reflections are markedly strengthened. The removal of 2.5 wt % H results in weakening of the broad peak and its shifting by  $\sim 0.8^\circ$  to larger angles, and this peak disappears after heating to 650°. The sharp graphite (002) and (004) reflections are retained and their intensity relative to the background changes only slightly. It was reported in the literature that an SWNT is not destroyed at hydrostatic pressures below 13 GPa [5]. For this reason, a change in the diffraction pattern of an SWNT after the thermal treatment in hydrogen should be assigned to the graphitization of amorphous carbon particles in the initial material and to the hydrogenation and dehydrogenation of a certain fraction of graphitized particles.

Weakly bonded hydrogen, which is released in an amount of less than 0.5 wt % upon heating to room temperature, can reasonably be assigned to physisorption, which is considered to be the dominant mechanism of hydrogen absorption by carbon materials at pressures below 12 MPa and not too high temperatures. To elucidate the nature of the bonded state of the main hydrogen mass that is retained up to high temperatures, the IR diffuse reflection spectra were measured for a GNF and SWNT in the initial state, after the treatment under hydrogen pressure, and after the degassing annealing.

Measurements were performed in the range 400–5000  $\text{cm}^{-1}$  at room temperature on a Bruker IFS-113v IR Fourier spectrometer. The results are presented in Fig. 3.

The diffuse reflection carries information primarily about the transmission spectrum of the sample [6]. The spectra of initial GNFs are characterized by a monotonic decrease in transmission with increasing photon energy; such a spectral behavior is typical of the spectra of purified nanotubes [7]. As in the case of nanotubes exhibiting properties of a strongly imperfect metal or semimetal, the light absorption by free charge carriers caused by their high-frequency conductivity is the most probable reason for a decrease in the GNF transmission with increasing photon energy. In the spectra of initial SWNTs, a broad transmission minimum near 2600  $\text{cm}^{-1}$  is superposed on the free-carrier absorption. Anomalies of this type were observed earlier and discussed in detail for granulated composite materials consisting of the conducting and nonconducting components (see [8] and references therein).

After the hydrogenation, the GNF transmission increases substantially over the entire range of measurements, and a narrow absorption band at 2860  $\text{cm}^{-1}$  with a halfwidth of 38  $\text{cm}^{-1}$  and a weaker band at 2920  $\text{cm}^{-1}$  appear in the spectrum. These energies are typical of the stretching C–H vibrations. In the spectra of hydrogenated SWNTs, the transmission also increases; an asymmetric band with a maximum at 2860  $\text{cm}^{-1}$  and a halfwidth of 95  $\text{cm}^{-1}$  appears in the spectrum, while the broad minimum disappears. The asymmetry of the SWNT C–H band can be explained by the overlap between the bands at 2860 and 2920  $\text{cm}^{-1}$ . The broad minimum irreversibly disappears in the subsequent annealing. Comparing with the changes in the SWNT diffraction pattern, one can assume that the minimum in the transmission spectrum of the initial SWNT is caused by the electric properties of the impurity amorphous carbon in the material, and the fact that it disappears is associated with the graphitization of carbon nanoparticles during the process of thermal treatment in hydrogen.

The disappearance of the C–H bands is the most pronounced effect in a partial (~40%) degassing of the GNF and SWNT samples. The background transmission is regained in part and occupies the intermediate position between the spectra of the initial and hydrogenated samples. After heating to 600–650  $^{\circ}\text{C}$  and removal of the main hydrogen mass, the spectra become somewhat closer to the spectra of initial samples, but no complete recovery occurs; the spectrum of the GNF annealed for 6 h in vacuum at 700 $^{\circ}\text{C}$  coincides with the spectrum observed after heating to 600 $^{\circ}\text{C}$  (curve 4).

The decrease in the free-carrier absorption upon hydrogenation can be associated with both decrease in the free-carrier concentration and increase in the rate of

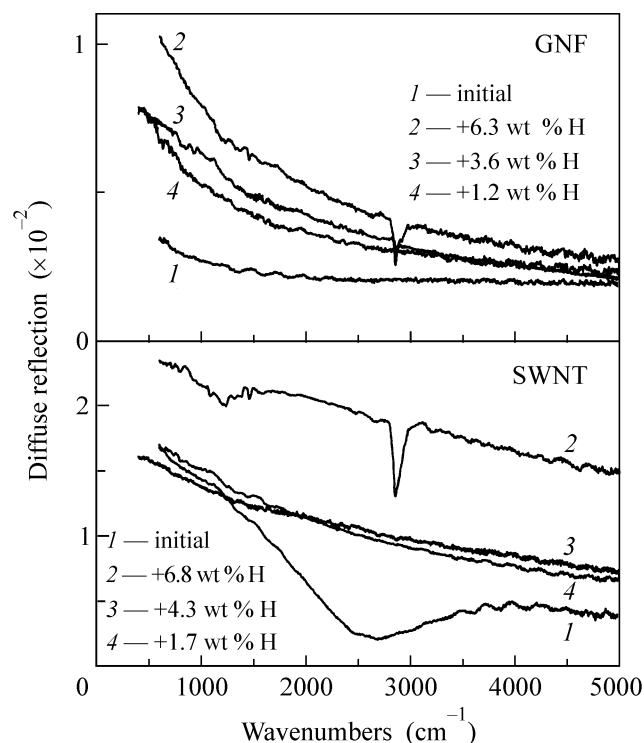


**Fig. 3.** IR diffuse reflection spectra of graphite nanofibers and single-walled carbon nanotubes: in the initial state, after saturation with hydrogen at 9 GPa, after removal of about 40% of absorbed hydrogen, and after degassing annealing. Room temperature.

their scattering from defects. After the conversion of the diffuse reflection spectra into the absorption spectra, we have found that, in the range of small wavenumbers  $\nu$ , the absorption changes as  $\sqrt{\nu}$ , which corresponds to the spectral dependence of free-carrier absorption in the Drude approximation for  $\nu$  much smaller than the charge-carrier scattering rate. By using the Drude relations, we found that, after the GNF and SWNT hydrogenation, the high-frequency free-carrier conductivity decreased by a factor of 9.

The combination of the experimental data gives evidence that there are three possible hydrogen states in the hydrogenated carbon nanostructures quenched under pressure. A small portion of hydrogen (less than 0.5 wt %) is retained at 77 K in the form of weakly bonded adsorbed molecules that are released below room temperature. About 40% of hydrogen retained up to room temperature forms strong C–H bonds that are thermally stable up to ~500 $^{\circ}\text{C}$ . However, 60% or more of the strongly bonded hydrogen occurs in the IR-inactive state. At a temperature of ~500 $^{\circ}\text{C}$ , hydrogen in this state is retained longer than the covalently bonded hydrogen. A change in the diffraction pattern of the multilayer GNF structure upon hydrogenation can be considered as being caused mainly by an increase in the lattice parameter  $c$ . In this case, the shift in the (002) peak after the absorption of 6.3 wt % H corresponds to

the increase in the interplanar spacing between the graphene layers by approximately 40% from 3.36 to 4.67 Å. The increase in  $c$  as large as that allows one to assume that the third state is a molecular hydrogen situated between the graphene layers in the nanofiber bulk. This assumption explains the two-phase diffraction pattern of the partially annealed GNF sample containing 3.6 wt % H, which is likely characterized by the presence of concentrational inhomogeneity and microstrains. The idea of accumulation of molecular hydrogen between the graphene layers was put forward earlier when studying the interaction of atomic hydrogen with graphite [9] or in the study of the interaction of hydrogen with graphite during the grinding process in ball mills [10, 11]. However, the diffraction measurements in these works were hampered by the fact that the penetrability of atomic hydrogen was limited by only one carbon layer [9], while the grinding in a mill rapidly brought the sample into the amorphous state [10, 11].

The question of the hydrogen positions in the hydrogenated SWNT product at normal conditions is more complicated. The possibility of hydrogen molecule penetrating through the wall of a closed SWNT was theoretically considered in [12]. However, one should take into account that our product contains from 40 to 50 wt % impurity carbon nanoparticles that crystallize upon thermal treatment and take part in the hydrogenation and dehydrogenation processes. All structure reflections in the SWNT diffraction patterns are likely caused by the presence of such (multilayer) particles in the hydrogenated or nonhydrogenated states. The hydrogen absorption by the SWNT product (6.8 wt % H, as compared to 6.3 wt % H in GNF), nevertheless, cannot be explained by the hydrogenation of impurity carbon particles alone, because they comprise the smaller part of the sample and are hydrogenated incompletely. It is reasonable to assume that the amounts of hydrogen in the carbon nanoparticles and in nanotubes themselves are comparable in the hydrogenated SWNT product. The fact that temperatures and desorption rates of hydrogen from the hydrogenated SWNT and GNF are close to each other allows one to assume that the bonding character between hydrogen and carbon in the SWNT and GNF, as well as the mechanism of hydrogen release, can be similar.

In summary, the interaction of carbon nanomaterials with hydrogen at high pressures and temperatures has given rise to thermally stable compounds containing up to 6.8 wt % of hydrogen, most of which is in the new state characterized by the absence of the C–H bands in the IR spectra.

This work was supported by the Russian scientific and technical program “Fullerenes and Atomic Clusters,” the program of OFN of the Russian Academy of Sciences “New Materials and Structures,” and the Russian Foundation for Basic Research (project no. 02-02-16859).

## REFERENCES

1. A. C. Dillon and M. J. Heben, *Appl. Phys. A* **72**, 133 (2001).
2. B. K. Pradhan, G. U. Sumanasekera, C. K. W. Adu, *et al.*, *Physica B (Amsterdam)* **323**, 115 (2002).
3. R. O. Loutfy, T. P. Lowe, J. L. Hutchison, *et al.*, in *Abstracts of IV Workshop on Fullerenes and Atomic Clusters (IWFA'99)* (St. Petersburg, 1999), p. 117.
4. V. E. Antonov, I. O. Bashkin, S. S. Khasanov, *et al.*, *J. Alloys Compd.* **330–332**, 365 (2002).
5. S. M. Sharma, S. Karmakar, S. K. Sikka, *et al.*, *Phys. Rev. B* **63**, 205417 (2001).
6. R. R. Willey, *Appl. Spectrosc.* **30**, 593 (1976); M. P. Fuller and P. R. Griffiths, *Anal. Chem.* **50**, 1906 (1978).
7. A. V. Bazhenov, V. V. Kveder, A. A. Maksimov, *et al.*, *Zh. Éksp. Teor. Fiz.* **113**, 1883 (1998) [*JETP* **86**, 1030 (1998)].
8. P. Sheng, *Phys. Rev. Lett.* **45**, 60 (1980).
9. E. A. Denisov, T. N. Kompaniets, I. V. Makarenko, *et al.*, *Materialovedenie* **2**, 45 (2002).
10. S. Orimo, T. Matsushima, H. Fujii, *et al.*, *J. Appl. Phys.* **90**, 1545 (2001).
11. T. Fukunaga, K. Itoh, S. Orimo, *et al.*, *J. Alloys Compd.* **327**, 224 (2001).
12. Y. Ma, Y. Xia, M. Zhao, *et al.*, *Phys. Rev. B* **63**, 115422 (2001).

*Translated by V. Sakun*